In-situ calibration of the water vapor channel for multi-filter rotating shadowband radiometer using collocated GPS, AERONET and meteorology data

In-situ calibration of the water vapor channel for multi-filter rotating shadowband radiometer using collocated GPS, AERONET and meteorology data

Maosi Chen, Melina-Maria Zempila, John M. Davis, Robert W. King, Wei Gao

Maosi Chen, Melina-Maria Zempila, John M. Davis, Robert W. King, Wei Gao, "In-situ calibration of the water vapor channel for multi-filter rotating shadowband radiometer using collocated GPS, AERONET and meteorology data," Proc. SPIE 9975, Remote Sensing and Modeling of Ecosystems for Sustainability XIII, 99750E (19 September 2016); doi: 10.1117/12.2236572

SPIE.

Event: SPIE Optical Engineering + Applications, 2016, San Diego, California, United States

In-situ calibration of the water vapor channel for Multi-Filter Rotating Shadowband Radiometer using collocated GPS, AERONET and meteorology data

Maosi Chen*[a], Melina-Maria Zempila [a], John M. Davis [a], Robert W. King [b], Wei Gao [a,c]
[a] UV-B Monitoring and Research Program, Natural Resource Ecology Laboratory, Colorado State University, 1304 S. Shields, Fort Collins, Colorado; [b] Department of Earth, Atmospheric and Planetary Sciences, Massachusetts Institute of Technology, Cambridge, Massachusetts; [c] Department of Ecosystem Science and Sustainability, Colorado State University, Fort Collins, CO 80521, USA

ABSTRACT

The difficulty of in-situ calibration on the 940 nm channel of Multi-Filter Rotating Shadowband Radiometer (MFRSR) stems from the distinctive non-linear relationship between the amount of precipitable water vapor (PW) and its optical depth (i.e. curve of growth) compared to the counterpart of aerosols. Previous approaches, the modified Langley methods (MLM), require exact aerosol optical depth (AOD) values and a constant PW value at all points participating the regression. Instead, we propose a new method that substitutes the PW optical depth derived from collocated GPS zenith wet delay retrieval in conjunction with meteorology data and requires a constant AOD value at all points participating the regression. The main benefits of the new method include: (1) Aerosol stability is easier to fulfill than PW stability; (2) AOD stability could be inferred from adjacent channels (e.g. 672 and 870 nm) of MFRSR itself without measurements of a collocated AERONET sun photometer; and (3) When applicable, there are no time gaps of GPS derived PW due to clouds and sun positions. Both MLM and the new method were applied to the MFRSR of USDA UV-B Monitoring and Research Program at the station in Billings, Oklahoma (active for 18 years so far) on July 28, 2015. The performances of the two methods are compared in order to assess their accuracy and their advantages and disadvantages.

Keywords: MFRSR, Water Vapor, 940 nm, GAMIT, GPS, Langley Calibration, MODTRAN

1. INTRODUCTION

The U.S. Department of Agriculture (USDA) UV-B Monitoring and Research Program (UVMRP) has being collecting solar radiation data in ultraviolet (UV), visible (VIS), and near-infrared (NIR) ranges at 36 climatology sites since 1992 [1]. Each UVMRP climatology site is equipped with a UV version and a VIS version of a Yankee Environmental Systems Inc. (YES) Multi-Filter Rotating Shadowband Radiometer (MFRSR), a YES broadband UVB-1 pyranometer, a photosynthetically active radiation (PAR) LI-COR sensor, and other ancillary data [1]. The measurements of these instruments are averaged at a 3-minute interval [1] and made accessible to the public through UVMRP website (http://uvb.nrel.colostate.edu/UVB/index.jsf) 36 hours after collection.

UVMRP uses the in-situ Langley methods to calibrate most UV and VIS MFRSR channels [1][2]. Water vapor absorption near 940 nm in narrow regions of the 10 nm wide band as the precipitable water vapor (PW) column increases. As a result, water vapor optical depth varies non-linearly (i.e. curve of growth) with PW column amount compared to the counterpart of aerosols [3]. Therefore, the original Langley method does not apply for the MFRSR 940 nm channel. The Modified Langley Method (MLM) was initially developed in 1980s to solve this problem [4][5]. The key assumption of MLM is that water vapor is stable during the calibration window, which is hard to assure in practice [3]. Such limitations can be avoided by applying the laboratory lamp calibration. However, lamp calibration is expensive and cannot be applied as frequently as in-situ calibrations due to limited laboratory resources.

Microwave signals such as those transmitted by the Global Positioning System (GPS) satellites are delayed by both the

* maosi.chen@colostate.edu; phone: 1-(970)491-3604

Remote Sensing and Modeling of Ecosystems for Sustainability XIII, edited by Wei Gao, Ni-Bin Chang, Proc. of SPIE Vol. 9975, 99750E · © 2016 SPIE · CCC code: 0277-786X/16/$18 · doi: 10.1117/12.2236572

hydrostatic ("dry") and water vapor ("wet") components of the atmosphere [6]. By combining the signals received at widely separated ground stations and removing the hydrostatic delay using local measurements of pressure, we can recover the wet delay and convert this to PW [7][8][9]. In addition, a wide range of ground instruments such as sunphotometers, lidar systems, microwave radiometers may provide precipitable water vapor measurements/retrievals [3][10]. These ground instruments are widely distributed, especially in the GPS network and Aerosol Robotic network, NASA (AERONET). Therefore, in this study, we propose a new method that is based on Beer's law equation but substitutes the water vapor transmittance term with one derived from the GPS delay or directly from the AERONET precipitable water vapor product. The new method requires concurrent meteorological measurements as well as the site-specific relationship between precipitable water and its transmittance determined by a radiative transfer model. The calibration results of the new method on a clear morning at one site with water vapor derived from collocated GPS or AERONET data are compared to those of the original Langley method and the Modified Langley Method.

2. DATA AND INSTRUMENTATION

2.1 The 940 nm MFRSR data

The VIS-MFRSR observes the direct normal, diffuse horizontal, and total horizontal solar radiation at 7 VIS channels with 10-nm FWHM (i.e. 415, 500, 610, 665, 870, and 940 nm) [1][2]. The collected raw data are transferred to and stored at the UVMRP database, where quality control (such as bad data identification, dark current removal, and cosine response correction) and calibration procedures are applied to ensure that the irradiance measurements are of the highest standard. Among the 7 MFRSR channels, the 940 nm channel is special because it is at a center of a water vapor absorption band and the normal Langley analysis/regression that applies to other channels is not directly applicable to this channel [3]. In this study, the UVMRP site to be investigated is at Billings, Oklahoma, OK01 (36.60 N, 97.49 W, 317 m). Collocated GPS and AERONET stations near OK01 provide water vapor and other atmospheric parameters for implementing and validating the new calibration method. The 3-minute cosine corrected voltage at 940 nm channel, and the associated ancillary data such as solar zenith angle are obtained for July 28, 2015 from the UVMRP database.

2.2 The GPS data and processing software

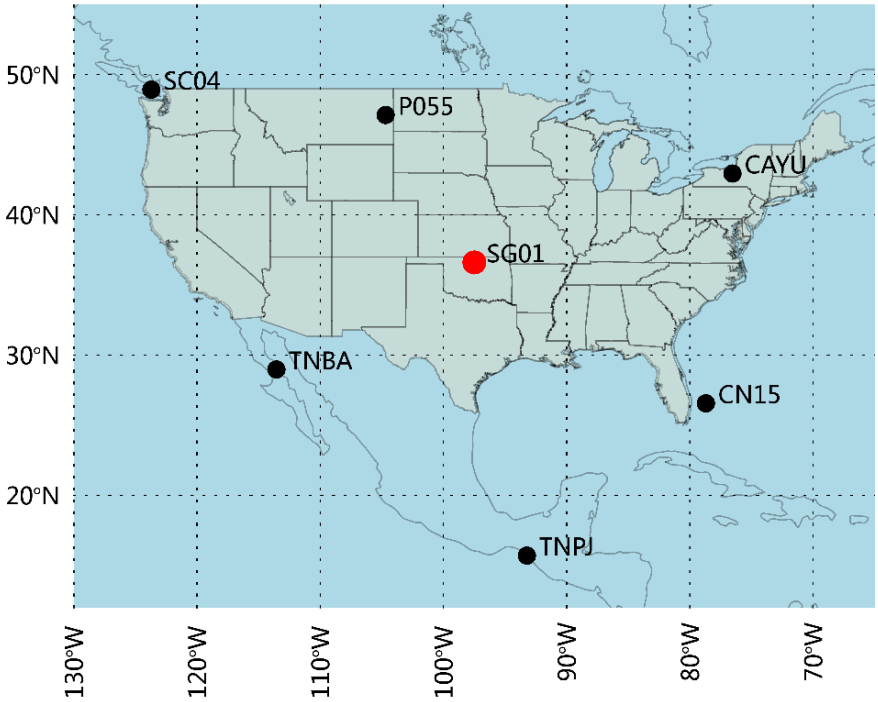

Figure 1. Spatial distribution of the GPS station (SG01, red solid circle) collocated with UVMRP OK01 site and six remote GPS stations (SC04, P055, CAYU, CN15, TNPJ, and TNBA, black solid circles) for solving the zenith delays at SG01.

For this study, we used 24-hour files of GPS phase and pseudorange observations from seven continuously operating tracking stations spread across North America (Figure 1) that are part of the National Science Foundation (NSF) sponsored Plate Boundary Observatory (http://pbo.unavco.org/; http://www.earthscope.org/science/observatories/pbo/) and equipped with meteorological packages. The main GPS station for this study is the SG01 station at University of Oklahoma, which is collocated with the UVMRP OK01 site. The six remote GPS stations in Sidney, Canada (SC04), Glendive, Montana (P055), Auburn, New York (CAYU), Freeport, Bahamas (CN15), Pijijiapan, Mexico (TNPJ), and Bahia De Los Angeles, Mexico (TNBA) are included to allow estimation of the absolute (and not just relative) values of the zenith wet delay parameters in the geodetic inversion [9].The GPS data as well as temperature and pressure measurements from the seven stations are available from the UNAVCO Data Center (http://www.unavco.org/data/gps-gnss/gps-gnss.html).

We processed the GPS data using the GAMIT software developed at the Massachusetts Institute of Technology (http://www-gpsg.mit.edu/~simon/gtgk/index.htm) [11] [12]. The software uses doubly differenced phase measurements and complex models for the motions of the satellite and ground stations in a least-squares inversion to estimate station coordinates and the atmospheric zenith total delay (ZTD) parameters for each station. The ZTD is modeled as a linear spline with knots at one-hour intervals. Although more tightly spaced knots can be used, the uncertainty of the ZTD estimates increases with fewer data available to constrain each parameter. The zenith wet delay (ZWD) and precipitable water vapor are extracted from the ZTD estimates in post-processing, as described in Section 3.3.1. The orbital positions of the satellites used in the processing are acquired in tabular form from the data centers of the International GNSS Service (IGS) (http://www.igs.org/) and are typically accurate to about 2 cm, sufficient for mm-level recovery of station coordinates and ZTDs.

2.3 The AERONET data

Water vapor retrievals are provided at the Cart_Site in Billings, Oklahoma by a CIMEL sun photometer that is part of the Aerosol Robotic Network (AERONET), NASA (http://aeronet.gsfc.nasa.gov/, [13]). The radiometer is programmed to obtain 2 basic measurements, either direct or sky, both in several alternate sequences. The direct sun measurements are provided in 8 spectral bands and require a time span of ~10 seconds. This type of measurements cover the UV, the visible and as well the near infrared spectral regions (340, 380, 440, 500, 670, 870, 940 and 1020 nm).

The quality assurance of the AERONET data is verified by the regular calibration of the instruments. Direct sun and radiance sphere calibration coefficients are measured at distributed calibration sites, while NASA GSFC is responsible of maintaining reference instruments that meet high operating standards and determining the extraterrestrial constants at Mauna Loa Observatory in Hawaii.

The 940 channel measurements are used to derive the columnar water abundance. The 940 channel calibration coefficients are determined by the modified Langley method [5][14]. The calibration coefficients are typically calculated from an average of five or more Langley plots while the variability of the retrieved mean calibration coefficient is expressed by the coefficient of variation (CV, standard deviation/mean) that indicates the combined uncertainty of the atmosphere, instrument and the repeatability of the calibration procedure. The averaged Mauna Loa calibration coefficient obtained during all calibration sessions have a CV of ~1 to 3% for the water vapor channel. The water vapor transmittance is then modeled from each 940 nm filter function using MODTRAN and has been proven to be quite independent of temperature and water vapor profiles [15].

3. METHODOLOGY

3.1 Beer's Law at 940 nm channel

The Beer-Bouguer-Lambert Law (i.e. Beer's Law) is a simplified approach to describe the relationship between the direct beam irradiances at top of the atmosphere and at ground via the atmospheric transmittance. The Beer's law has been used to calibrate the MFRSR and the CIMEL sun-photometer and to retrieve the atmospheric components retrieval from their direct-beam measurements [13][16][17]. The atmospheric transmittance at most channels is expressed as the exponential of negative airmass multiplied by total optical depth. In the transformed Langley coordinate system [18], the vertical distance between a measurement and the virtual top-of-atmosphere line represent that measurement's total optical depth. In that coordinate system, a measurement's y value or its optical depth changes linearly with the column density of the atmospheric components (e.g. aerosol and molecules other than water vapor) at all airmasses. However, at the 940 nm

channel, the frequent strong water vapor absorption lines results in a different pattern (i.e. power function) than a linear pattern between precipitable water vapor column and water vapor optical depth. Therefore, the transmittance terms for water vapor and other atmospheric components should be expressed separately in Beer's Law equation [5][4][10]:

$$V_t(940) = V_{LO}(940) \cdot e^{-m_t \cdot (\tau_{RL,t} + \tau_{A,t})} \cdot T_{w,t}(940), \quad (1)$$

where,
$V_t(940)$ denotes the measured MFRSR voltage at 940 nm channel at time *t*.
$V_{LO}(940)$ is the corresponding voltage as if it is measured at the top of the atmosphere. Note that $V_{LO}(940)$ here is the raw value derived for a particular day, which varies with sun-earth distance during the year.
m_t is the relative optical air mass at time *t*, which is a function of solar zenith angle (θ_t in degrees) [19][10]:

$$m_t = \left(\cos\theta_t + 0.15 \cdot (93.885 - \theta_t)^{-1.253}\right)^{-1}.$$

$\tau_{RL,t}$ and $\tau_{A,t}$ are the Rayleigh and aerosol optical depth at 940 nm channel at time *t*, respectively.
$T_{w,t}(940)$ is the slant path water vapor transmittance at 940 nm channel at time *t*, which can be depicted by a power function [3][10]:

$$T_{w,t}(940) = \exp\left(-a(m_{w,t} \cdot PW_t)^b\right), \quad (2)$$

where,
$m_{w,t}$ is the relative water vapor airmass [20]:

$$m_{w,t} = \left(\cos\theta_t + 0.031141 \cdot \theta_t^{0.1} \cdot (92.4710 - \theta_t)^{-1.3814}\right)^{-1}.$$

Note that the parameter 0.031141 in Gueymard 2001 is different from the value (0.311141) reported in Pérez-Ramírez et al. 2012.
PW_t is the precipitable water vapor in vertical column (in unit cm) at time *t*.

The coefficients *a* and *b* vary with the MFRSR's spectral response function at 940 nm channel, as well as the atmospheric pressure-temperature lapse rate and the vertical distribution of water vapor [15][3][10]. Nevertheless, the common values of *a* and *b* should be around 0.5 or 0.6 [3]. Alternatively, the relation between $T_{w,t}(940)$ and $m_{w,t} \cdot PW_t$ (i.e. the slant path precipitable water vapor) can be depicted by more complicated functions including piece-wise linear functions.

In order to create the lookup table between the slant-path precipitable water vapor and slant-path water vapor transmittance (the curve of growth) at the Billings, Oklahoma (Cart_Site/SG01/OK01) site, the MODTRAN v5.3 radiative transfer model was used (http://modtran5.com/, [21][22]). For cases where explicit relationship between column water vapor and slant-path water vapor transmittance is required, the two coefficients (*a* and *b*) were also calculated at the site. The lookup table is mainly for the newly developed calibration method, while the two coefficients are mainly for the modified Langley method.

For the execution of the MODTRAN model, the following key parameters were included: standard atmospheric profile (in card 1), transmittance mode (in card 1), 1 cm^{-1} band model (in card 1A2), no cloud and standard aerosol profile (in card 2), site altitude (in cards 2 & 3), solar zenith angle (in card 3), spectral range and resolution (in card 4). Note that MODTRAN reports water vapor in unit of atm cm at standard temperature and pressure (STP), it is converted to the more common unit of g cm^{-2} (or cm) by the equation: 1 g cm^{-2} = 1.244E+3 cm atm STP [23].

3.2 Modified Langley Method (MLM)

The Modified Langley Method (MLM) has been widely discussed in the literature [4][5][3] for calibrating the 940 nm channel in radiometers using its direct beam measurements. The MLM first combines and rearranges Eq. (1) and (2):

$$\ln V_t(940) + m_t \cdot (\tau_{RL,t} + \tau_{A,t}) = \ln V_{LO}(940) - a(m_{w,t} \cdot PW_t)^b. \quad (3)$$

Then, MLM proposes three requirements/assumptions on Eq. (3):
(a) $\tau_{RL,t}$ and $\tau_{A,t}$ during the whole calibration period are known;
(b) the two coefficients (*a* and *b*) at the site should be obtained; and
(c) PW_t during the whole calibration period are low and stable.

The requirement (a) is satisfied by the following procedures. Using a fitted "ratio of polynomials" function [24], $\tau_{RL,t}$ can be simulated when surface pressure at site is known. For the Cart_Site, the surface pressure measurements are provided by AERONET. $\tau_{A,t}$ can be interpolated or extrapolated from adjacent calibrated MFRSR channels (e.g. 870 nm channel). For a collocated MFRSR and AERONET site, $\tau_{A,t}$ can be also provided by the latter. The $\tau_{A,t}$ at 940 nm channel can be obtained from $\tau_{A,t}$ at adjacent CIMEL channels by interpolation in the $\ln(\tau_{A,t})$-$\ln(\lambda)$ coordinate system [25].

The way to fulfill the requirement (b) has been discussed in the section 3.1.

The assumption (c) is hard to meet at most sites [3] except for some very dry places like the Arctic [26] or high mountains [27].

When all three requirements and assumptions are met, the only unknown terms in Eq. (3) are $V_{LO}(940)$ and the average of PW_t during the calibration period. Similar to the original Langley method, one can use linear regression on Eq. (3) to solve both of them together. $\ln V_{LO}(940)$ is the regression intercept and $-a(PW_t)^b$ is the regression slope.

3.3 New Langley method with PW removal

The limitation of MLM's applicability stems from the water vapor stability assumption. If precipitable water vapor is measured/retrieved with some collocated instrument, then the slant path water vapor transmittance can be obtained via the modeled curve of growth. It is observed that when the airmass is large, the two-coefficient parameterization [i.e. Eq. (2)] is not very accurate [3]. Therefore, the piece-wise linear function was applied to fit the curve of growth. Furthermore, if the aerosol value is still available through a collocated AERONET site, then $V_{LO}(940)$ can be directly calculated from Eq. (1) without regression. In cases where collocated aerosol measurements are not available, $V_{LO}(940)$ can be retrieved with the original Langley regression, assuming the stability of AOD over calibration period:

$$\ln\left(\frac{V_t(940)}{T_{w,t}(940)}\right) = \ln\left(V_{LO}(940)\right) - m_t \cdot (\tau_{RL,t} + \tau_{A,t}), \tag{4}$$

or with the transformed Langley regression [18]:

$$m_t^{-1} \cdot \ln\left(\frac{V_t(940)}{T_{w,t}(940)}\right) = m_t^{-1} \cdot \ln\left(V_{LO}(940)\right) - (\tau_{RL,t} + \tau_{A,t}) \ , \tag{5}$$

where, $\tau_{RL,t} + \tau_{A,t}$ together (i.e. total optical depth excluding water vapor optical depth) is treated as one unknown variable, and $V_{LO}(940)$ is the other unknown variable. In the transformed Langley plot [Eq. (5)], the regression slope denotes $\ln V_{LO}(940)$ and the y-intercept denotes the average of $-(\tau_{RL,t} + \tau_{A,t})$. The stability of aerosol and Rayleigh optical depth at 940 nm channel can be ensured by the calibrated 870 nm channel of MFRSR. The absolute value of Rayleigh optical depth at 940 nm channel is small and its variation within a day at a site due to surface pressure change is also small. Since the AOD stability assumption is relatively easier to fulfill than the water vapor stability assumption, given that precipitable water vapor is available, the new calibration method for the 940 nm channel is as applicable as the original/transformed Langley calibration method on other MFRSR channels.

A wide range of ground instruments may provide precipitable water vapor measurements/retrievals: sunphotometers, radiosondes, lidar systems, microwave radiometers, and global positioning system (GPS) receivers [3][10]. An agreement with average difference of precipitable water vapor less than 2.2% was reported among the three methods (i.e. AERONET, GPS, and High Resolution Limited Area Model [HIRLAM]) [28]. In this study, we choose GPS as the preferred water vapor source for its large station distribution, availability under virtually all weather conditions, independency of sun position, no need for calibration, accuracy comparable to radiosonde, and relatively low cost [29][30]. The AERONET water vapor product is used to validate the retrieved GPS water vapor as well as to compare the $V_{LO}(940)$ retrieved by the new method using GPS or AERONET water vapor.

3.3.1 GAMIT GPS water vapor retrieval

Once the motions the satellites and ground stations are modeled in the analysis of observations, there are three propagation delays to be accounted for: the delay introduced by the ionosphere and neutral atmosphere, and signal scattering due to reflections from nearby surfaces (multipath) and the antenna structure itself. The first-order ionospheric delay is inversely proportional to the transmission frequency and is removed by appropriate combination of the two GPS frequencies. Second- and third-order effects are usually not modeled but are negligible for meteorological studies under most ionospheric conditions [31]. The neutral atmosphere delay is not dispersive at GPS frequencies thus has to be modeled or estimated in the analysis. The "dry" component comprised of gases in hydrostatic equilibrium can be modeled precisely using only measurements of surface pressure. Since water vapor is not in hydrostatic equilibrium, its delay is poorly represented by surface measurements and must be estimated with other parameters in the analysis. Signal scattering is also difficult to model and is minimized by careful antenna design and averaging over long observation spans. It is typically the largest source of error in PW recovery using GPS.

The total delay accumulated along the signal path with satellite elevation angle, $D(\theta_{GPS})$, is related to the two zenith delays by the hydrostatic and wet mapping functions that relate the observed path ("slant") delay to the delay at the zenith [7][9][11]:

$$D(\theta_{GPS}) = ZHD \cdot DRYMAP(\theta_{GPS}) + ZWD \cdot WETMAP(\theta_{GPS}) \ , \quad (6)$$

where, θ_{GPS} is the satellite elevation angle, $DRYMAP(\theta_{GPS})$ is the hydrostatic mapping function, $WETMAP(\theta_{GPS})$ is the wet mapping function. The hydrostatic zenith delay is given by [32]:

$$ZHD = 10^{-6} \frac{k_1 R_d}{g_m} P_{sfc} \ , \quad (7)$$

where, P_{sfc} is the surface pressure, g_m is the mean gravity, k_1 = 77.604 K hPa^{-1} is the refractivity constant for dry air, and R_d = 287.04 J K^{-1} kg^{-1} is the specific constant for dry air [33]. From Eq. (7), a 1 mbar error in surface pressure implies an error of ~2 mm in ZHD, equivalent to ~0.3 mm in PW.

From Eq. (6), we see that the mapping functions become the partial derivatives used in the estimation of zenith delay from the delay along the signal path sensed by the observations. Since the differences between the dry and wet mapping functions are too small to estimate the ZHD and ZWD separately, we assume that ZHD has been adequately modeled and use the wet mapping function as the partial derivative in estimating the adjustment to the a priori ZTD. If there is residual error in the ZHD, this error will propagate into the ZWD adjustments at a level of ~0.15 mm/mbar [34], or ~ 0.02 mm/mbar in PW. Since this sensitivity of the a priori ZHD is an order of magnitude less than the direct sensitivity of the ZWD to the pressure measurement, we do not need to use the pressure measurements in the GAMIT processing (though the software allows this), but rather can use the more convenient pressure values extracted from global numerical weather models and stored on a 0.25° spatial grid at 6-hr intervals by the Technical University of Vienna [35]. The mapping functions themselves depend on pressure and temperature, so we take these also from the Vienna grid files, designated VMF1.

The quantity of column precipitable water can be related to ZWD at the GPS receiver by [8]:

$$PW = \Pi \times ZWD \ , \quad (8)$$

where, Π is a dimensionless constant of proportionality [36], which is a function of the weighted mean temperature of the atmosphere (T_m) [37][8]:

$$\Pi = 10^6 \left[\rho_w R_v \left(k_3 / T_m + k_2^{'} \right) \right]^{-1} , \quad (9)$$

where, ρ_w is the density of dry air; R_v is the gas constant for water vapor; k_2' = (17 ± 10) K mbar^{-1}; k_3 = (3.776 ± 0.004) x 10^5 K^2 mbar^{-1}. $T_m = \int (P_v / T) dz \Big/ \int (P_v / T^2) dz$. T_m can be estimated either from numerical weather prediction models or from surface temperature with the relative error of less than ~1% and ~2%, respectively [7][8]. In addition, Jade et al. 2005 found that various empirical relationships between surface temperature and mean weighted atmosphere temperature agree within ±1 mm deviation in India [38].

In summary, for this study we estimated ZTD from the GPS observations between 0h and 24h UTC on July 28, 20 using a linear spline at 1-hour intervals with the knots loosely constrained to vary by 2 cm/sqrt(hr) and the a priori ZHD and mapping functions read from a VMF1 grid derived from a global numerical weather model. We then interpolated the ZTD values from the linear spline at 3-minutes intervals, corrected the a priori (VM1) ZHD using pressure measurements from the stations, also linearly interpolated at 3-minute intervals, and subtracted the corrected ZHD from ZTD to obtain ZWD. We then used Eq. (9) with a value of T_m computed from the surface temperature at the station.

4. RESULTS AND DISCUSSION

4.1 The lookup table for curve of growth and the fitting coefficients

The PW is treated as an unknown value and to be solved via linear regression in the modified Langley method, which means when applying the MLM, the water vapor transmittance has to be expressed as function as PW in Eq. (2) explicitly. The values of the two coefficients in Eq. (2), *a* and *b*, were 0.48 and 0.52 for the MFRSR 940 nm channel at OK01 site on July 28, 2015, respectively (Table 1). Since the actual atmospheric profile of the date of investigation over OK01 site is unknown, its sensitivity was tested on 3 standard atmospheric profiles (i.e. 1976 U.S. standard [USS], mid-latitude summer [MLS], and mid-latitude winter [MLW]). The results showed that the difference of the water vapor transmittance between USS and MLS is less than 0.0070 within the PW range [0.0, 15.0] cm; and the difference between MLW and USS is less

than 0.0035 within the same PW range. Besides, since the simulation results at all solar zenith angles were used together to create one lookup table for any slant path water vapor amount, the sensitivity of simulated slant path water vapor transmittance on solar zenith angle was also tested. The result showed that for precipitable water vapor less than 2.5 cm there was a -0.00024 to 0.00146 deviation on slant path water vapor transmittance in solar zenith angle range of [0, 80] degrees compared to those at the 40 degree; for precipitable water vapor less than 5.0 cm there was a -0.00024 to 0.00016 deviation on slant path water vapor transmittance in solar zenith angle range of [65, 80] degrees compared to those at the 72 degree. Compared to the uncertainty or variation of aerosol and Rayleigh transmittance at the site, the uncertainties discussed above are negligible. The lookup table between slant path PW and slant path water vapor transmittance at OK01 site on July 28, 2015 is presented in Figure 2. The distribution of PW values from AERONET at Cart_Site (OK01) in 2015 ranged from 0.3 to 4.6 with the mean value at 1.7 cm. With the maximum airmass currently allowed for Langley regression (i.e. 5.0), the maximum slant path water vapor is 23.0. Therefore, the lookup table range of 0.0 to 25.0 covered all possible points for Langley calibration.

Table 1. The coefficients *a* and *b* of the "curve of growth" determined by the MODTRAN radiative transfer model and the spectral response function of the MFRSR 940 nm channel at the UVMRP OK01 site (Billings, Oklahoma) on July 28, 2015.

a	0.480664
b	0.517992

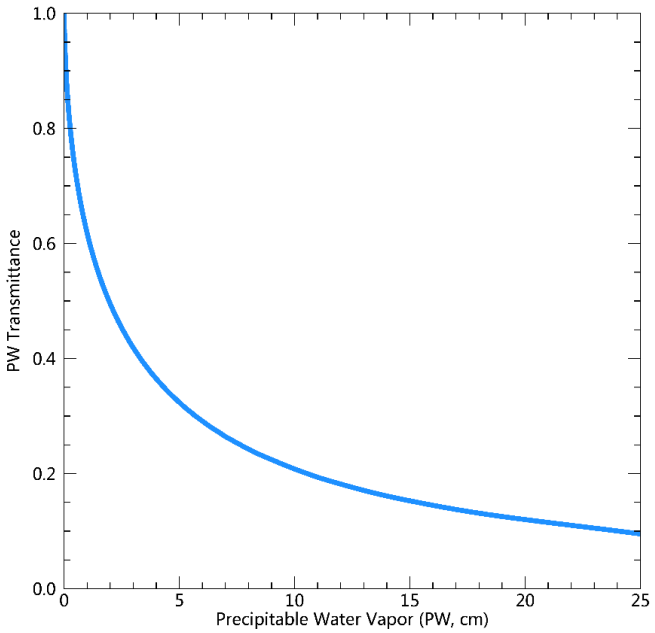

Figure 2. The lookup table/function between slant path precipitable water vapor and the corresponding direct transmittance for the UVMRP MFRSR 940 nm channel at OK01 on July 28, 2015.

4.2 Comparison of the precipitable water vapor retrieved from two sources

The AERONET PW is derived from sun-photometer measurements, which require that the sun is directly visible to the instrument. This means that during the nighttime or cloudy periods, there will be no PW values from AERONET. On the other hand, GPS satellites broadcast signals at much longer wavelength, which means when the ground station can receive the GPS signal, the PW can be retrieved at any time under most weather conditions. For our MFRSR 940 nm channel calibration, the nighttime advantage of GPS is not important since MFRSR also only works when sun is visible. However, the advantage of GPS to work under almost all weather condition is important for the new calibration method especially when there are broken clouds because the interpolated/extrapolated AERONET PW during intermittent clear-sky periods may not be accurate.

Generally, on the morning of July 28, 2015, PW from GAMIT GPS and AERONET agreed with each other with less than 0.1 cm deviation (Figure 3). Both PW sources showed a relatively stable status (PW: 2.7-2.8 cm) between 12:30 – 15:30 UTC (i.e. 6:30 am - 9:30 am local time) and an increasing trend (PW: 2.8->3.2) between 15:30 and 18:00 UTC (i.e. 9:30 am – noon local time). Figure 4 showed a scatter plot between AEROENT PW and GAMIT GPS PW on the same morning at time matching measurements. The linear regression between the two PW sources gave an R^2 of 0.9442 and a y-intercept of 0.2541 cm.

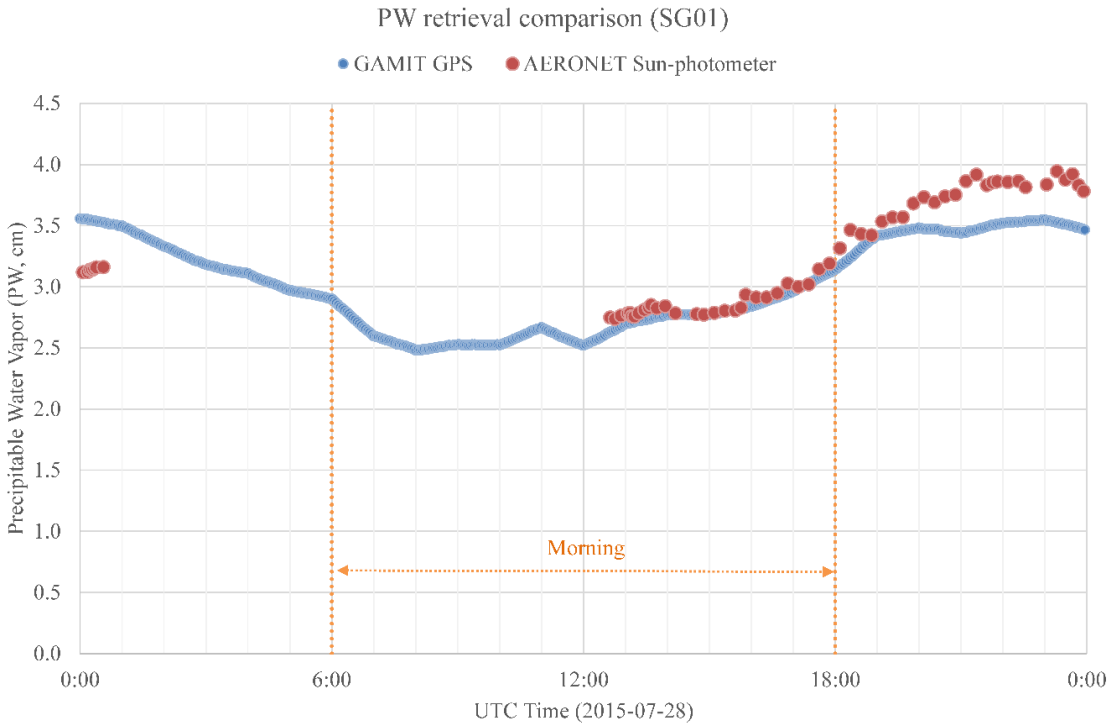

Figure 3. Time series of precipitable water vapor retrieved from GPS by GAMIT (blue circles every 3 minutes) and obtained from AERONET (v1.5) (red circles at 15-minute intervals) at the collocated GPS SG01 and AERONET Cart_Site sites (in Billings, Oklahoma) on UTC day July 28, 2015. The local morning period is highlighted by dashed orange lines. The time zone of the site is -6 (Central Standard Time).

However, the persistent bias for about 5 hours between 19:00-24:00 UTC and 1 hour between 0:00-1:00 UTC (Figure 3) needs further investigation. It is difficult to conclude which PW source is more accurate without additional data. The first and last hour of the UTC day in the GAMIT linear-spline formulation have a larger uncertainty, ~0.25 cm in this case, but this cannot be the cause of the differences between 17:00-22:00. Other potential sources of GPS errors, either in the ZTD recovery or the conversion of ZTD to PW using surface measurements of P and T do not seem to be large enough to explain a 0.5 cm difference. An error in the AERONET-derived PW seems more likely. Holben et al. 2001 estimated the uncertainty of AERONET-derived PW to be around 10% [39]. Another comparison between HIRLAM, GPS, and AERONET showed that the AERONET method overestimated PW by 5–9% at PW < 12 mm and underestimated it by 6–10% at PW > 25 mm [28].

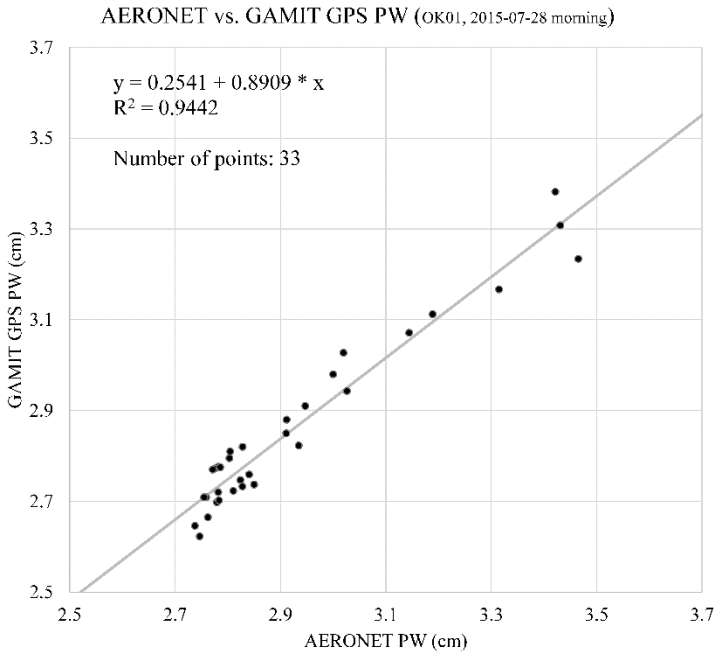

Figure 4. The scatter plot of precipitable water vapor from GPS by GAMIT and from AERONET on the morning of July 28, 2015 at the collocated GPS SG01 and AERONET Cart_Site sites (in Billings, Oklahoma).

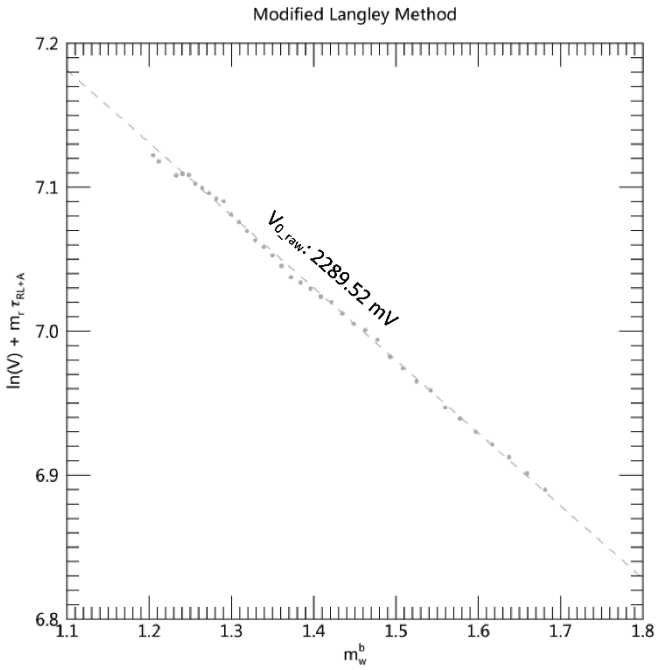

Figure 5. The plot of the modified Langley method (MLM) at UVMRP OK01 site (in Billins, Oklahoma) on the morning of July 28, 2015. The meanings of the variables m_w, b, τ_{RL}, and τ_A have been described for Eq. (2) and Eq. (3). The value of b is reported in Table 1. There are 37 points participating the MLM regression. The aerosol optical depths of these points obtained from AERONET ranged from 0.0448 to 0.0492. The Rayleigh optical depths on these points ranged from 0.010948 to 0.010950. The MLM $V_{LO}(940)$ (raw and normalized to average sun-earth distance) are reported in Table 2.

4.3 MLM

Even though Figure 3 suggested that the assumption of stable water vapor during calibration for MLM was violated on the morning of July 28, 2015, the MLM was still applied to investigate its effects on the calibration factor. Figure 5 displayed the 940 nm measurements with aerosol and Raleigh optical depth removed as well as the regression line in the MLM coordinate system (y axis: $\ln V(940)+m\ (\tau_{RL}+\tau_A)$; x axis: m_w^b) on the same morning. Among the 37 points participating the MLM regression, 6 of them were excluded as regression outliers. The aerosol optical depths of these points obtained from AERONET range from 0.0448 to 0.0492. The Rayleigh optical depths on these points ranged from 0.010948 to 0.010950. It is seen in Figure 5 that even with the increasing water vapor, the points still distributed along a line. This means that the $V_{LO}(940)$ derived from MLM on the morning was biased. Since the slope of MLM regression line represents $-a(PW)^b$ (a monotonic decreasing function of column water vapor) and column water vapor increased as m_w^b decreased on the morning, it is expected that the slope of the line with the same amount of column water vapor should be steeper, which means the true $V_{LO}(940)$ should be higher than the one reported by the MLM (see Table 2). The variation of water vapor during a short time window like this case is common at Billings, Oklahoma (i.e. OK01/Cart_Site), which suggests that the MLM is not suitable to be applied as a routine in-situ calibration method at the site.

4.4 The new and original Langley calibration methods

The new 940 nm channel Langley calibration was performed on the same morning of July 28, 2015 at the OK01 site in the transformed Langley coordinate system [18]. In the transformed Langley system, the V_{o_raw} [the raw $V_{LO}(940)$ from the Langley regression] is the exponential of the slope of the Langley regression.

The total optical depth on the adjacent MFRSR 870 nm channel on the morning was calculated to find the stable points for calibrating the 940 nm channel after removal of the water vapor transmittance. In our case, 37 points having the most stable total optical depth (i.e. within the range of [0.11335, 0.11770]) at the 870 nm channel were selected.

The measurements before removing the slant path water vapor transmittance are displayed as grey points in the plot [Figure 6 (a)]. After the water vapor removal (GAMIT GPS was used as the PW source; the MODTRAN lookup table converted PW into the corresponding slant path water vapor transmittance), they are the blue points in the plot [Figure 6 (a)]. It is seen that the vertical distance between each pair of points (before and after water vapor removal), or the expression $a\ m^{b-1}\ PW^b$ (the difference between m and m_w is ignored here), increased as the reciprocal of airmass (m^{-1}) increased. Although the variation of column water vapor also showed the same pattern as m^{-1} increased (or as time increased in the morning), the main reason for this increasing deviation is for a constant PW, a~0.5, and b~0.5, as m^{-1}increases, m decreases, m^{b-1}increases, and $a\ m^{b-1}\ PW^b$ increases. It is also the reason for the significant difference (85.27%) of V_{o_raw} between the new method and the original Langley method when the Langley regressions were applied.

Table 2. List of V_{o_raw} [the raw $V_{LO}(940)$ from the Langley regression] and V_{o_norm} (the V_{o_raw} that is normalized to average sun-earth distance) on July 28, 2015 at OK01/Cart_Site/SG01 from the original Langley method, the modified Langley method, and the new Langley method with the PW from GAMIT GPS and from AERONET products. The percent differences of V_{o_raw} (or V_{o_norm}) of various methods compared to the original Langley method are reported in the last column.

		V_{o_raw} (mV)	V_{o_norm} (mV)	% difference of V_{o_raw} (or V_{o_norm}) compared to the original Langley method
Original Langley method		1634.58	1685.50	-
Modified Langley method		2289.52	2360.84	40.07
Langley method with PW removal	PW source: AERONET	2903.34	2993.78	77.62
	PW source: GAMIT GPS	3028.32	3122.66	85.27

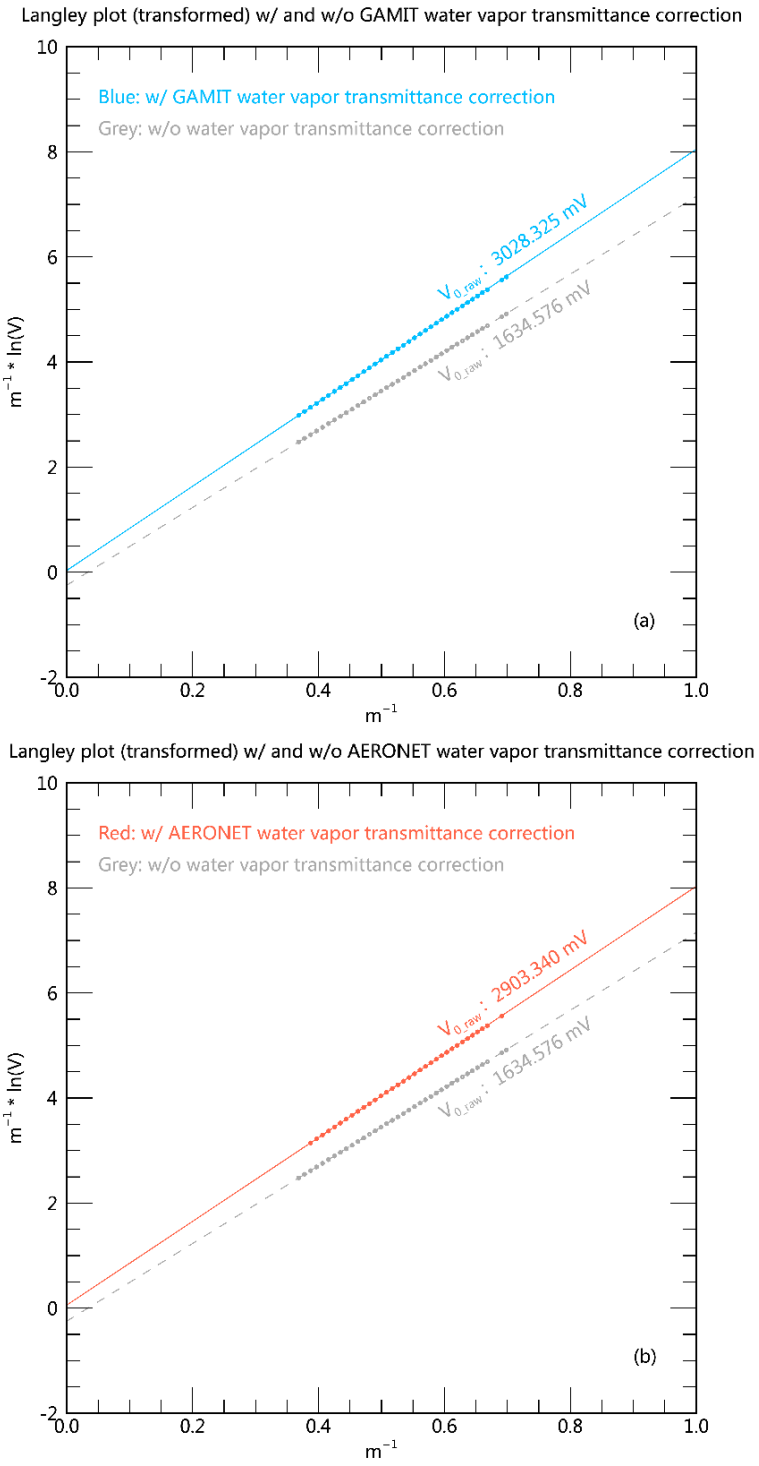

Figure 6. The new 940 nm channel Langley calibration method with precipitable water vapor provided from GAMIT GPS retrieval (a) and AERONET (b). Both regressions were performed on the transformed Langley coordinates. The grey solid circles denote the original measurements; the blue and red solid circles denote the adjusted measurements with slant water vapor transmittance from GAMIT GPS retrieval and AERONET removed from the corresponding original measurements, respectively. The dashed (grey) line represents the Langley regression on the original measurements. The blue and red lines represent the Langley regressions on the GAMIT GPS and AERONET adjusted measurements, respectively. The new methods' $V_{LO}(940)$ (raw and normalized to average sun-earth distance) using the two water vapor sources are reported in Table 2.

The new method using GAMIT GPS as PW source [Figure 6 (a), blue symbols] and using AERONET as PW source [Figure 6 (b), red symbols] showed similar but slight different calibration results (V_{o_raw} was 3028.325 mV for GAMIT GPS and 2903.340 mV for AERONET). One explanation could be that they were obtained via Langley regression on slightly different data points. It is noted that when choosing the AERONET PW, 3 less points participated in the new method's Langley regression than when choosing the GPS GAMIT PW. The reason is that extrapolation of the AERONET PW was not allowed in order to limit the uncertainty. Another explanation may have to do with the dependency of the vertical distance on m^{b-1} discussed in previous paragraph. Although the PW difference between the two sources was small on the morning of calibration (i.e. less than 0.1 cm, Figure 3), the relative difference of the two V_{o_raw}s was magnified (i.e. to 4.3%) due to this dependency.

Table 2 summarized the 940 nm channel Langley offsets derived from the original Langley method, the modified Langley method, and the new Langley method with the PW from GAMIT GPS and from AERONET products on July 28, 2015 at OK01. The original Langley method showed the significant lower V_{o_raw} than the other two methods, which illustrates that ignoring the specialty of the 940 nm channel and performing the Langley regression can result in inaccurate calibration. Although the stable PW assumption was not met, the modified Langley method showed 40.07% higher V_{o_raw} than the original Langley method. However, the analysis in section 4.3 suggested that the true V_{o_raw} should be higher. The new Langley method either using PW from GAMIT GPS or from AERONET showed significant higher V_{o_raw} than the other two methods. When the stable total optical depth assumption is fulfilled and the site-specific curve of growth or the lookup table is available, the new method should be better than the other two methods. However, without knowing the true calibration value (e.g. from a laboratory lamp calibration) and extended application in the field, it is too early to make a definite conclusion as to the accuracy and uncertainty of the new calibration method.

5. CONCLUSIONS

The strength of water vapor absorption varies dramatically near 940 nm. Therefore, unlike most atmospheric constituents (e.g. aerosol and non-absorptive gaseous molecules) whose column amounts are related to the slant path optical depths as linear functions of airmass, the water vapor has such relationship with its slant path optical depth as a non-linear function of airmass (i.e. curve of growth). As a result, the original Langley calibration method is not directly applicable on the MFRSR 940 nm channel. The modified Langley method solves the problem with the additional PW stability assumption and independent aerosol and Rayleigh optical depth from collocated instruments. This study explored an alternative approach that removes the slant path water vapor transmittance and calibrates the 940 nm channel as other MFRSR channels with a Langley regression. In this study, the slant path water vapor transmittance was calculated using the PW retrieved from GPS by the GAMIT software or from the AERONET product and the site specific lookup table between PW and its slant path transmittance from the radiative transfer model MODTRAN. The PW retrieved from GAMIT GPS agreed with the AERONET PW product at the 0.1 cm level on the morning of July 28, 2015 at Billings, Oklahoma. The performance of the original Langley method, the modified Langley method, and the new method was compared at the same site and in the same time period. The new method showed significantly higher calibration factor than the other two methods, suggesting the importance of removing water vapor on the 940 nm channel calibration. Validation of PW retrieval using the GAMIT software and the new calibration method at more sites and for longer time periods is necessary in the future study.

ACKNOWLEDGEMENTS

This work is supported by the USDA NIFA projects (2014-34263-22038) and (2015-34263-24070), and at MIT by NSF grant S13-EAR1261833-S4 and NASA grant NNX14AQ03G. We thank Rick Wagener for its effort in establishing and maintaining the Billings, Oklahoma AERONET site.

REFERENCES

[1] Bigelow, D. S., Slusser, J. R., Beaubien, A. F., and Gibson, J. H., "The USDA Ultraviolet Radiation Monitoring Program," Bulletin of the American Meteorological Society 79(4), 601-615 (1998).

[2] Chen, M., Davis, J., Sun, Z., and Gao, W., "Two-stage reference channel calibration for collocated UV and VIS Multi-Filter Rotating Shadowband Radiometers," Proc. SPIE 9610, 96100L (2015).

[3] Alexandrov, M. D., Schmid, B., Turner, D. D., Cairns, B., Oinas, V., Lacis, A. A., Gutman, S. I., Westwater, E. R., Smirnov, A., and Eilers, J., "Columnar water vapor retrievals from multifilter rotating shadowband radiometer data," J. Geophys. Res. 114, D02306 (2009).

[4] Reagan, J. A., Thome, K., Herman, B., and Gall, R., "Water vapor measurements in the 0.94 micron absorption band: Calibration, measurements, and data applications," Proceedings, International Geoscience and Remote Sensing Symposium, '87 Symposium, IEEE, 63-67 (1987).

[5] Bruegge, C. J., Conel, J. E., Green, R. O., Margolis, J. S., Holm, R. G., and Toon, G., "Water vapor column abundance retrievals during FIFE," J. Geophys. Res. 97, 18759-18768 (1992).

[6] Businger, S., Chiswell, S. R., Bevis, M., Duan, J., Anthes, R. A., Rocken, C., Ware, R. H., Exner, M., VanHove, T., and Solheim, F. S., "The Promise of GPS in Atmospheric Monitoring," Bulletin of the American Meteorological Society 77(1), 5-18 (1996).

[7] Bevis, M., Businger, S., Herring, T. A., Rocken, C., Anthes, R. A., and Ware, R., "GPS meteorology: Remote sensing of atmospheric water vapor using the Global Positioning System," J. Geophys. Res. 97, 15787-15801 (1992).

[8] Bevis, M., Businger, S., Herring, T. A., Anthes, R. A., Rocken, C., and Ware, R., "GPS meteorology: Mapping zenith wet delays onto precipitable water," J. Appl. Meteorol. 33, 379-386 (1994).

[9] Duan, J., Bevis, M., Fang, P., Bock, Y., Chiswell, S., Businger, S., Rocken, C., Solheim, F., van Hove, T., Ware, R., McClusky, S., Herring, T. A., and King, R. W., "GPS Meteorology: Direct Estimation of the Absolute Value of Precipitable Water," J. Appl. Meteorol. 35(6), 830-838 (1996).

[10] Pérez-Ramírez, D., Navas-Guzmán, F., Lyamani, H., Fernández-Gálvez, J., Olmo, F. J., and Alados-Arboledas, L., "Retrievals of precipitable water vapor using star photometry: Assessment with Raman lidar and link to sun photometry," J. Geophys. Res. 117, D05202 (2012).

[11] Herring, T. A., King, R. W., and McKlusky, S. C., "GAMIT Reference manual GPS Analysis at MIT, Release 10.6," Department of Earth, Atmospheric, and Planetary Sciences, Massachusetts Institute of Technology, Boston, (2015).

[12] Herring, T. A., King, R. W., Floyd, M. A., and McKlusky, S. C., "Introduction to GAMIT/GLOBK," Department of Earth, Atmospheric, and Planetary Sciences, Massachusetts Institute of Technology, Boston, (2015b).

[13] Holben, B. N., Eck, T. F., Slutsker, I., Tanré, D., Buis, J. P., Setzer, A., Vermote, E., Reagan, J. A., Kaufman, Y. J., Nakajima, T., Lavenu, F., Jankowiak, I., and Smirnov, A., "AERONET - A Federated Instrument Network and Data Archive for Aerosol Characterization," Remote Sensing of Environment 66(1), 1-16 (1998).

[14] Reagan, J. A., Thome, K. J., and Herman, B. M., "A simple instrument and technique for measuring columnar water vapor via Near-IR differential solar transmission measurements," IEEE Trans. Geosci. Remote Sensing 30, 825-831 (1992).

[15] Halthore, R. N., Eck, T. F., Holben, N. B., and Markham, B. L., "Sunphotometric measurements of atmospheric water vapor," J. Geophys. Res. 102, 4343-4352 (1997).

[16] Chen, M., Davis, J., Tang, H., Gao, Z., and Gao, W., "A multi-channel calibration method for multi-filter rotating shadow-band radiometer," Proc. SPIE 8513, 851305 (2012).

[17] Chen, M., Davis, J., Tang, H., Ownby, C., and Gao, W., "The calibration methods for Multi-Filter Rotating Shadowband Radiometer: A review," Frontiers of Earth Science 7(3), 257–270 (2013).

[18] Chen, M., Davis, J., and Gao, W., "A New Cloud Screening Algorithm for Ground-Based Direct-Beam Solar Radiation," Journal of Atmospheric and Oceanic Technology 31(12), 2951-2605 (2014).

[19] Kasten, F., and Young, A. T., "Revised optical air mass table and approximation formula," Appl. Opt. 28, 4735-4738 (1989).

[20] Gueymard, C. A., "Parameterized transmittance model for direct beam and circumsolar spectral irradiance," Sol. Energy 71, 325-346 (2001).

[21] Anderson, G. P., Berk, A., Acharya, P. K., Bernstein, L. S., Adler-Golden, S. M., Lee, J., and Muratov, L., "Reformulated Atmospheric Band Model Method for Modeling Atmospheric Propagation at Arbitrarily Fine Spectral Resolution and Expanded Capabilities," U.S. Patent, 7593835 (2009).

[22] Berk, A., Anderson, G. P., Acharya, P. K., Bernstein, L. S., Muratov, L., Lee, J., Fox, M., Adler-Golden, S. M., Chetwynd, J. H., Hoke, M. L., Lockwood, R. B., Gardner, J. A., Cooley, T. W., Borel, C. C., Lewis, P. E., and Shettle, E. P., "MODTRAN5: 2006 Update," Proc. SPIE 6233, 62331F (2006).
[23] Liang, S., [Quantitative Remote Sensing of Land Surfaces]. Wiley, Hoboken, 225-225 (2004).
[24] Bodhaine, B. A., Wood, N. B., Dutton, E. G., and Slusser, J. R., "On Rayleigh optical depth calculations," J. Atmos. Oceanic Technol. 16, 1854-1861 (1999).
[25] Krotkov, N., Bhartia, P. K., Herman, J., Slusser, J., Labow, G., Scott, G., Janson, G., Eck, T. F., and Holben, B., "Aerosol ultraviolet absorption experiment (2002 to 2004), part 1: ultraviolet multifilter rotating shadowband radiometer calibration and intercomparison with CIMEL sunphotometers," Optical Engineering 44(4), 041004 (2005).
[26] Kiedron, P., Michalsky, J., Schmid, B., Slater, D., Berndt, J., Harrison, L., Racette, P., Westwater, E., and Han, Y., "A robust retrieval of water vapor column in dry Arctic conditions using the rotating shadowband spectroradiometer," J. Geophys. Res., 106, 24007-24016 (2001).
[27] Schmid, B., Spyak, P. R., Biggar, S. F., Wherli, C., Sekler, J., Ingold, T., Matzler, C., and Kampfer, N., "Evaluation of the applicability of solar and lamp radiometric calibrations of a precision sun photometer operating between 300 and 1025 nm," Appl. Opt. 37, 3923-3941 (1998).
[28] Keernik, H., Ohvril, H., Jakobson, E., Rannat, K., and Luhamaa, A., "Column water vapour: an intertechnique comparison of estimation methods in Estonia," Proc. of the Est. Acad. of Sci. 63(1), 37-47 (2014).
[29] Gutman, S. I., Chadwick, R. B., Wolfe, D. E., Simon, A. M., Van Hove, T., and Rocken, C., "Toward and operational water vapor remote sensing system using GPS," FSL Forum, Forecast Systems Laboratory, 13-19 (1994).
[30] Gutman, S. I., Sahm, S. R., Benjamin S. G., and Schwartz, B. E., "Rapid retrieval and assimilation of ground based GPS precipitable water observations at the NOAA Forecast Systems Laboratory: Impact on weather forecasts," J. Meteorol. Soc. Jpn. 82(1B), 1-10 (2004).
[31] Fritsche, M., Dietrich, R., Knofel, C., Rulke, A., Vey, S., Rothacher, M., and Steigenberger, P., "Impact of higher-order ionospheric terms on GPS estimates," Geophys. Res. Lett. 32, L23311 (2005).
[32] Saastamoinen, J., [The Use of Artificial Satellites for Geodesy], American Geophysical Union, Washington, D.C., 247-251 (1992).
[33] Bosser, P., Bock, O., Pelon, J., and Thom, C., "An improved mean-gravity model for GPS hydrostatic delay calibration," IEEE Geoscience and Remote Sensing Letters 4(1), 3-7 (2007).
[34] Tregoning, P., and Herring, T. A., "Impact of a priori zenith hydrostatic delay errors on GPS estimates of station heights and zenith total delays," Geophy. Res. Let. 33, L23303 (2006).
[35] Böhm, J., Werl, B., and Schuh, H., "Troposphere mapping functionsfor GPS and Very Long Baseline Interferometry from European Centre for Medium-Range Weather Forecasts operational analysis data," J. Geophys. Res. 111, B02406 (2006).
[36] Jade, S., and Vijayan M. S. M., "GPS-based atmospheric precipitable water vapor estimation using meteorological parameters interpolated from NCEP global reanalysis data," J. Geophys. Res. 113, D03106 (2008).
[37] Davis, J. L., Herring, T. A., Shapiro, I. I., Rogers, A. E., and Elgered, G., "Geodesy by radio interferometry: Effects of atmospheric modeling errors on estimates of baseline length," Radio Sci. 20, 1593-1607 (1985).
[38] Jade, S., Vijayan M. S. M., Gaur, V. K., Prabhu, T., and Sahu, S. C., "Estimates of precipitable water vapor from GPS data in Indian subcontinent," J. Atmos. Sol. Terr. Phys. 67(6), 623-635 (2005).
[39] Holben, B. N., Tanré, D., Smirnov, A., Eck, T. F., Slutsker, I., Abuhassan, N., Newcomb, W. W., Schafer, J. S., Chatenet, B., Lavenu, F., Kaufman, Y. J., Vande Castle, J., Setzer, A., Markham, B., Clark, D., Frouin, R., Halthore, R., Karneli, A., O'Neill, N. T., Pietras, C., Pinker, R. T., Voss, K., and Zibordi, G., "An emerging ground-based aerosol climatology: aerosol optical depth from AERONET," J. Geophys. Res. 106, 12067-12097 (2001).